Constitutive Models & Computational Tools to Describe The Response of Materials For High Temperature Operating Conditions

K. R. Rajagopal (PI)

Texas A&M University

I. Joga Rao (Co-PI)

New Jersey Institute of Technology

Saradhi Koneru

Graduate Student, Texas A&M University

Grant # DE-FG26-06NT42714

Outline

- For material system (Ni based single crystal superalloys)
  - Task 1
    - Develop constitutive equations
  - Task 2
    - Implement into computational program (ABAQUS)
  - Task 3
    - Iterative scheme to optimize design

Introduction

Objective: To develop constitutive models for materials operating at high temperatures: modern single crystal superalloys.

- The model development will lead to better predictive capability of the response of single crystal turbine blades
- Better creep characteristics of single crystal superalloys and better design will lead to enhanced efficiency of gas turbines
- Approach can be used for other materials as well.

Introduction

- Higher inlet temperature ➔ higher efficiency, low fuel costs
- Last 3 decades – turbine airfoil temperature capacity has increased on an average by 4 ^{o}F per year
- Contribution to the increased temperature capacity
  ~ 40 % due to advanced materials (single crystal superalloys)

Introduction

- Single crystal superalloys have complex thermo-mechanical response
  - Modeling the response of such materials

  - It is expected that a constitutive model will
    - optimize the efficiency in design of components w.r.t preventing failure and preventing over design

    - eliminate the need for performing specimen tests for all component conditions (Huge savings in terms of cost and time!)

A Typical Creep Curve

- Stages of Creep

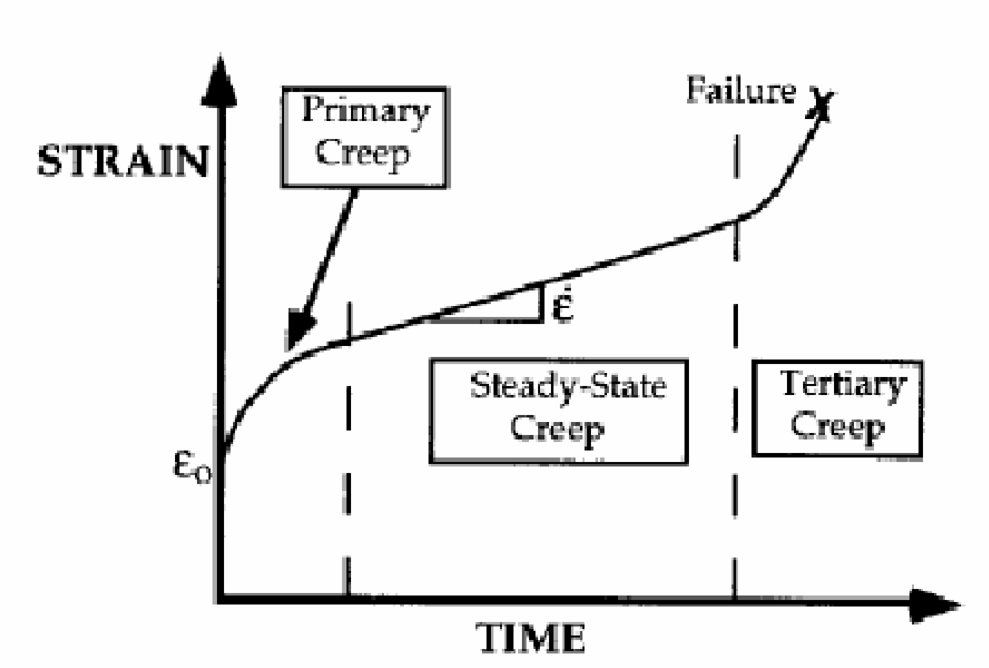

A typical creep curve

Creep of Nickel Superalloys Relationship to Microstructure

1. Characteristics of creep

   a. Single crystal has the longest creep life

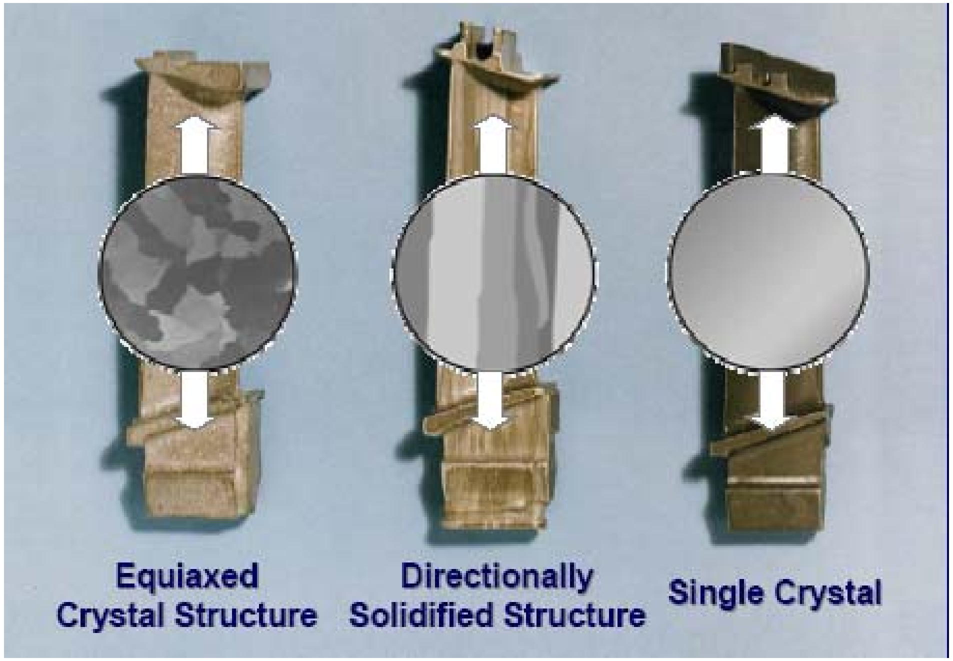

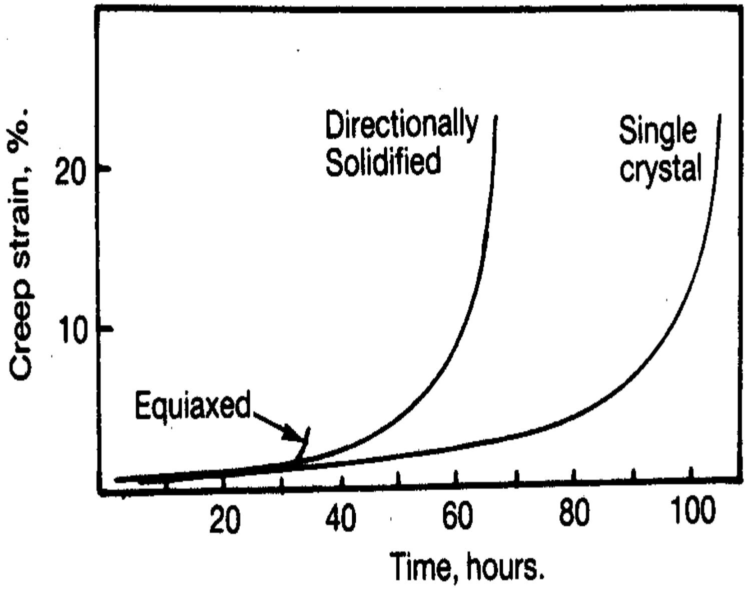

Factors Affecting Creep

2. Factors that affect the creep life

a. γ' volume and size
b. Misfit
c. Rafting
d. Orientation
e. Temperature and stress

Microstructure of Nickel Based Single Crystal Superalloy

γ’volume and size

Peak value: 70-80%
Size: 0.4-0.5μ m

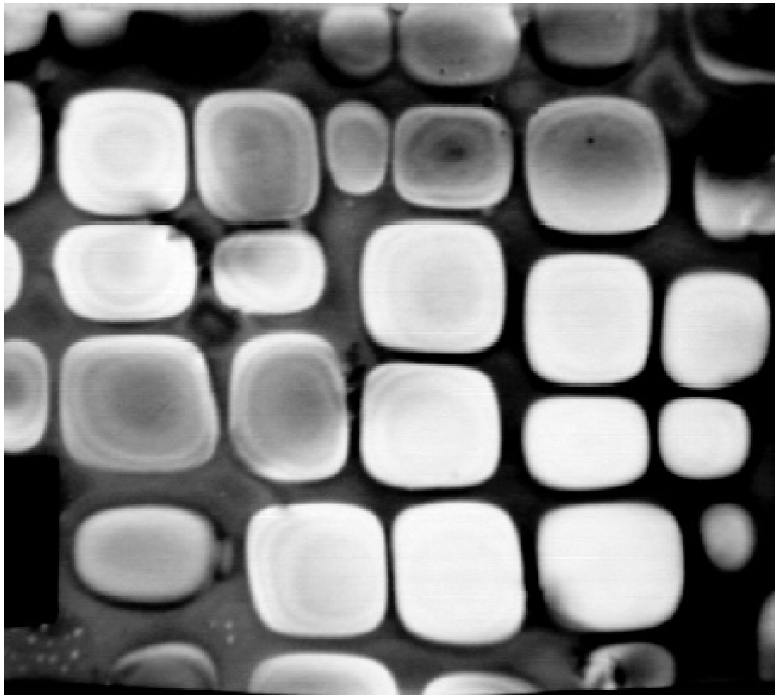

TEM photography of Nickel based single crystal superalloy SC16

Microstructure of Nickel Based Single Crystal Superalloy

Lattice misfit

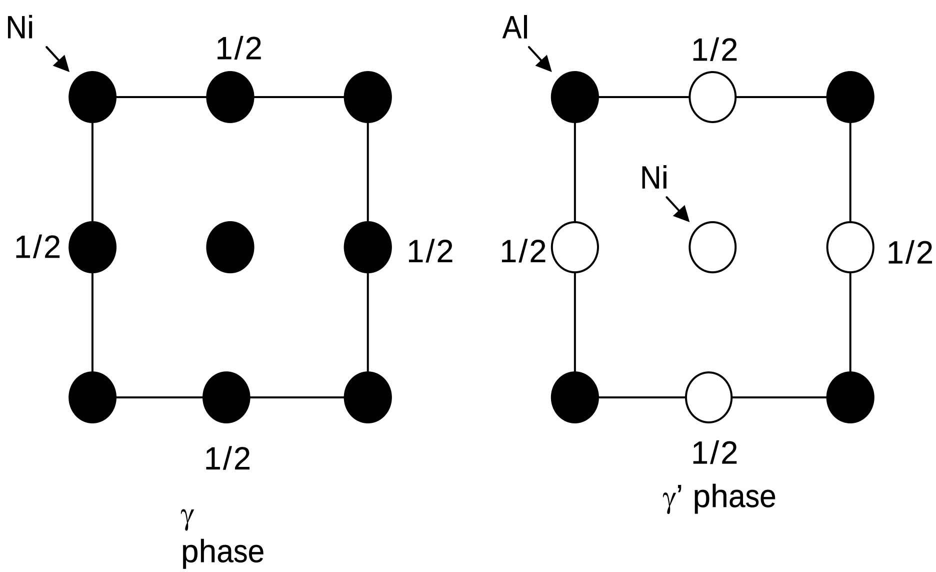

γ and γ' cell projections

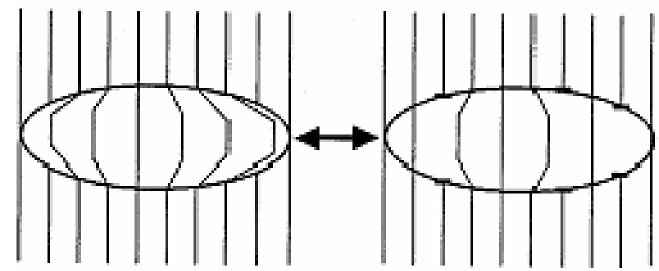

coherence incoherence

Schematic plot of coherence

Maximum creep rupture life when the misfit is a small fraction of 1% and when volume fraction of γ' is as high as possible. (Decreasing the misfit from 0.2% to zero led to a 50x increase in creep rupture life!)

Directional Coarsening of γ’

3. Rafting: directional coarsening of γ’

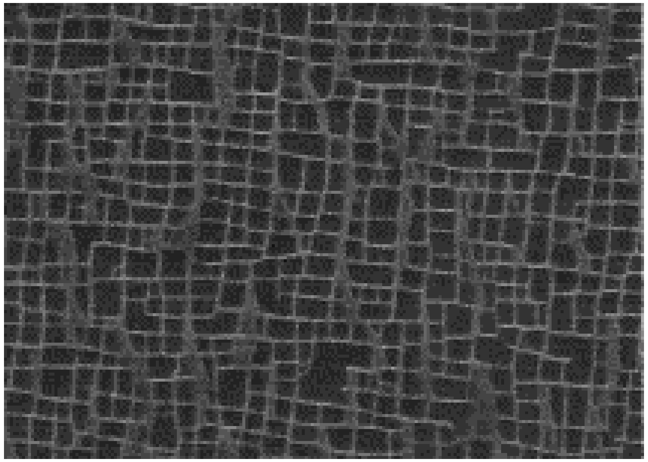 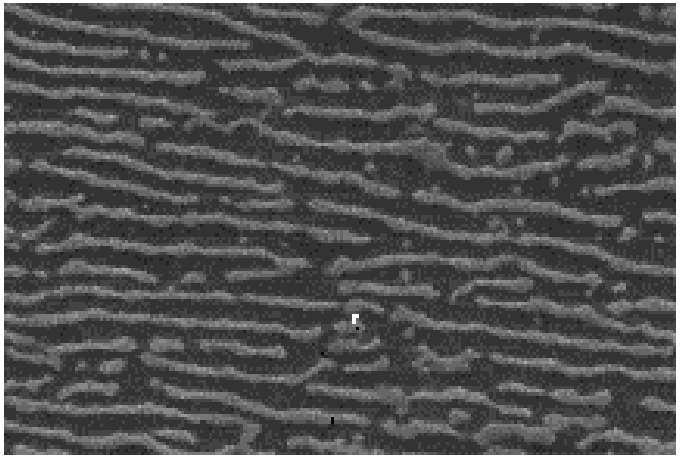

Microstructure changes during creep

The γ’ precipitates coarsen (Ostwald ripening) very slowly, because of the low interfacial energy between the γ and γ’

Anisotropic Creep

Creep is highly anisotropic

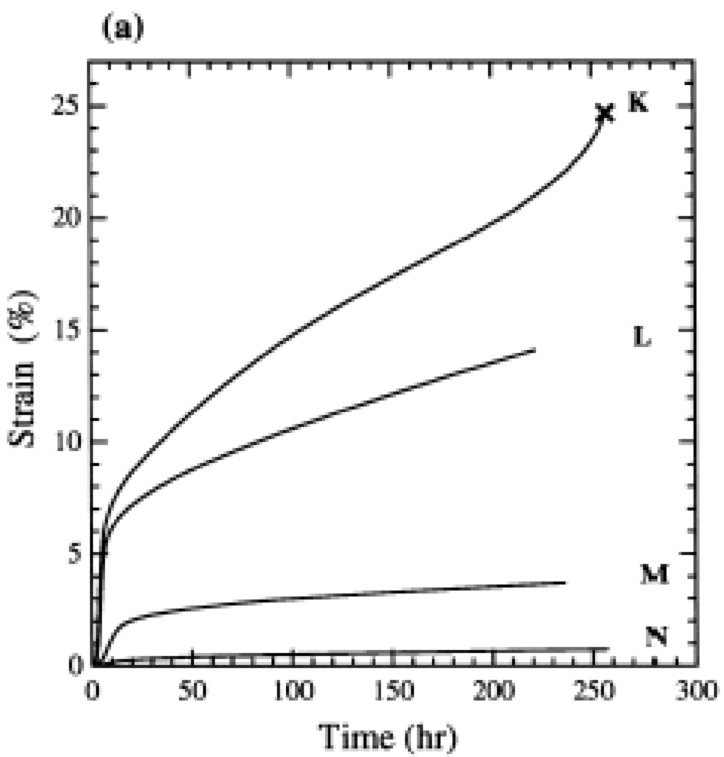

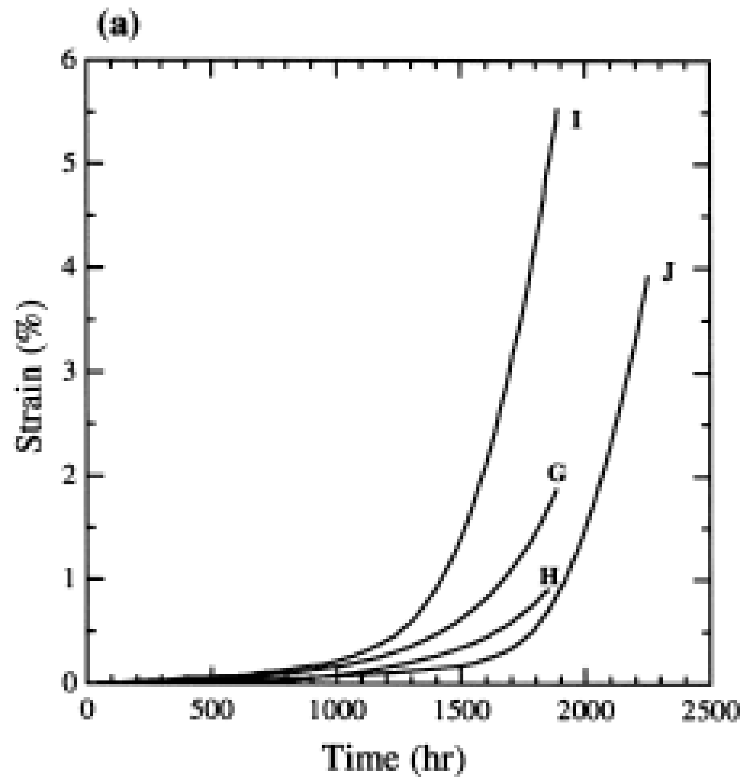

Creep for different orientations

750 ^{0}C

From Matan et al. (1999)

950 ^{0}C

Development of Constitutive Equations

- Use the theory of multiple natural configurations, as a crystal can exist stress free in more than one configuration.
- Develop a consistent thermodynamic setting, utilizing the maximization of rate of dissipation to obtain evolution equations for the natural configurations.
- Incorporate main features described: Anisotropy, Temperature dependence and microstructural effects, in an averaged manner.

Multiple Natural Configurations

- A body can possess many natural configurations;
- Response is elastic from these configurations.
- Evolution of underlying natural configuration has to be prescribed.

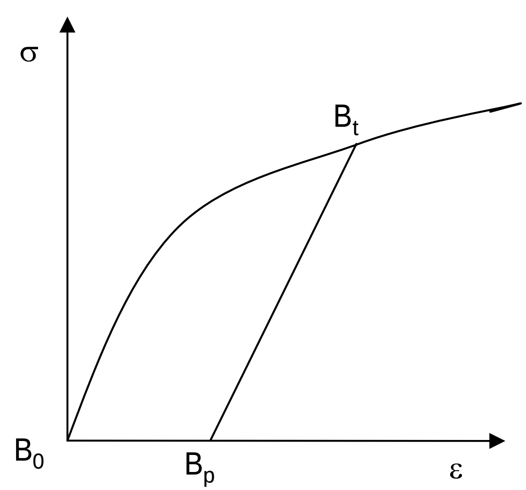

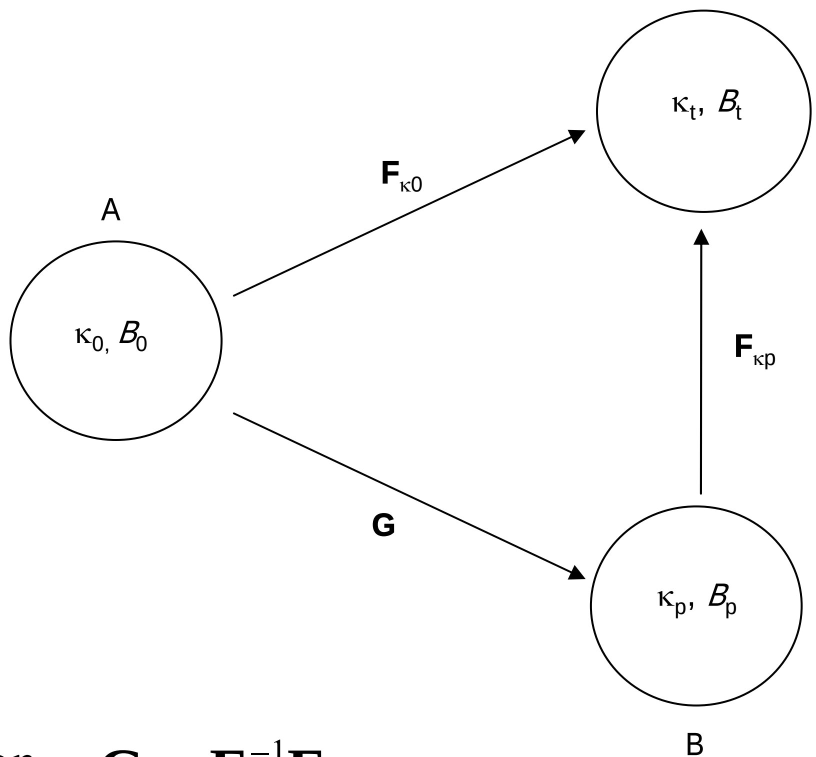

Evolution of the natural configuration $\mathbf{G} = \mathbf{F}_{\kappa_p}^{-1}\mathbf{F}_{\kappa_0}$

Natural configurations associated with single crystals

- Anisotropy associated with underlying crystal structure

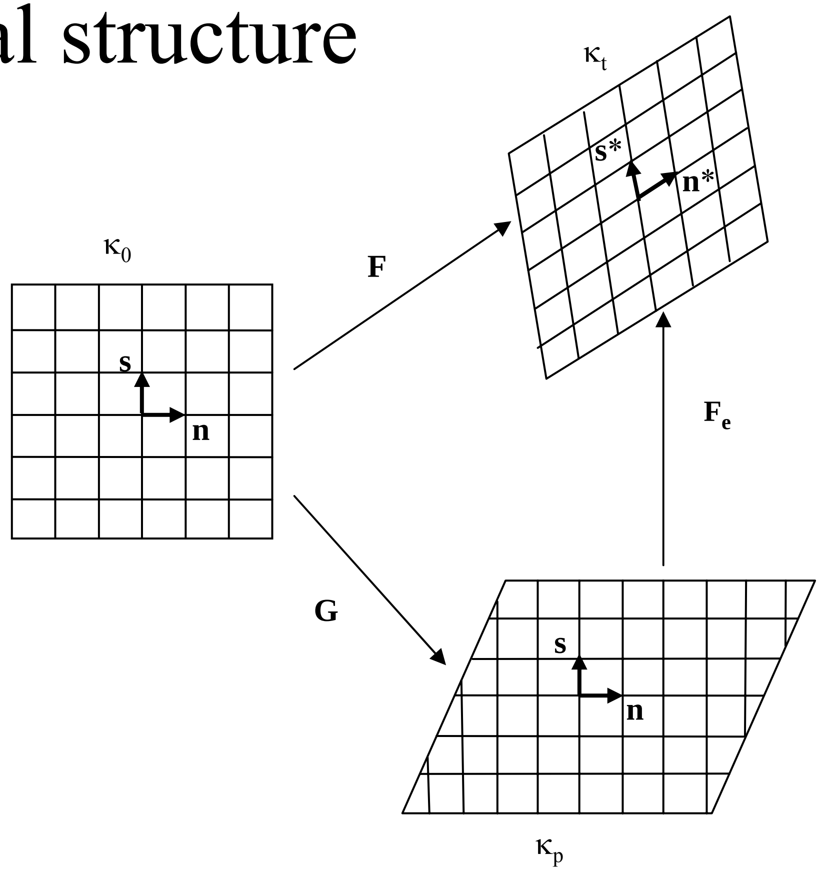

Model Development

- Second Law (Reduced Energy Dissipation Equation)

$$\mathbf{T.L} - \rho\dot{\psi} - \rho\eta\dot{\theta} - \frac{\mathbf{q}.\mathrm{grad}\,\theta}{\theta} = \rho\theta\xi := \zeta \geq 0$$

- After Simplification

$$\mathbf{T.L} - \rho\dot{\psi} = \zeta_{mech} \geq 0$$

- Need to prescribe constitutive equations for the:
  - Stored Energy ψ
  - Rate of Dissipation ζ

Model Development

- Stored Energy

$$\psi = \psi(\mathbf{F}_e, \mathbf{G})$$

- On Simplification, stress is obtained as

$$\mathbf{T} = 2\rho \mathbf{F}_\mathrm{e} \frac{\partial \psi}{\partial \mathbf{C}_e} \mathbf{F}_e{}^T$$

- Second Law reduces to

$$\mathbf{A}.\mathbf{D}_p + \boldsymbol{\tau}.\mathbf{W}_p - \rho \frac{d\tilde{\psi}}{dt} = \zeta_{mech} \geq 0,$$

$$\mathbf{A} = (\mathbf{F}_e^T \mathbf{T} \mathbf{F}_e^{-T})_{sym} \qquad \boldsymbol{\tau} = (\mathbf{F}_e^T \mathbf{T} \mathbf{F}_e^{-T})_{skew}$$

Specific Forms for Stored Energy

- Total stored energy is split:

$$\psi = \hat{\psi}\left(\mathbf{F}_e\right) + \tilde{\psi}\left(\mathbf{G}\right)$$

- Elastic Part

$$\hat{\psi} = \frac{1}{\rho}\mathbf{E}_{\boldsymbol{e}}.\mathbf{C}\mathbf{E}_e$$

$$\mathbf{C} = \begin{pmatrix} c_{11} & c_{12} & c_{12} & 0 & 0 & 0 \\ c_{12} & c_{11} & c_{12} & 0 & 0 & 0 \\ c_{12} & c_{12} & c_{11} & 0 & 0 & 0 \\ 0 & 0 & 0 & c_{44} & 0 & 0 \\ 0 & 0 & 0 & 0 & c_{44} & 0 \\ 0 & 0 & 0 & 0 & 0 & c_{44} \end{pmatrix}$$

Fourth order elasticity tensor for a FCC crystal

Inelastic Stored Energy

- Two main energy storage mechanisms (Mollica, Srinivasa and Rajagopal (2001))
- Energy stored in dislocation networks
- Use a dislocation density *a(s)* that depends on the inelastic strain path length, *s*

$$\dot{s} = \left\| \mathbf{D}_p \right\|; \quad s = \int_0^t \left\| \mathbf{D}_p \right\| d\tau$$

$$a(s) = a_o\left(1 + \beta_2\left(1 - e^{-\alpha_1 s}\right)\right)$$

- Based on experimental observations:
  - Dislocation density increases with inelastic deformation.
  - It reaches a saturation point.

Inelastic Stored Energy (contd)

- Second storage mechanism is due to the presence of the second hard γ’ phase.
- Dislocations face significant resistance to their motion.
- In particular they can get pinned
- Based on the work of Mollica et al. (2001)

$$\tilde{\psi} = \psi_1 \underbrace{a(s)}_{\text{Dislocation Networks}} + \psi_2 \underbrace{\int_0^s e^{\eta(x-s)} \left(\mathbf{E}_p(s) - \mathbf{E}_p(x)\right) \bullet \mathbf{N}(x) dx}_{\text{Resistance due to second phase}}$$

Inelastic Stored Energy (contd)

$$\rho \frac{d\tilde{\psi}}{dt} = h(s)(\mathbf{D}_p.\mathbf{D}_p)^{\frac{1}{2}} + \boldsymbol{\alpha}.\mathbf{D}_p,$$

$$\boldsymbol{\alpha} = \rho\psi_2 \int_0^s e^{\eta(x-s)} \mathbf{N}(x)dx, \quad \mathbf{N} = \frac{\mathbf{D}_p}{\sqrt{\mathbf{D}_p.\mathbf{D}_p}}$$

$$h(s) := \rho\left[\psi_1\left(a' + \eta a\right) - \eta\tilde{\psi}\right], \text{ Hardening}$$

$$\dot{\boldsymbol{\alpha}} = \rho\psi_2\mathbf{D}_p - \eta(\mathbf{D}_p.\mathbf{D}_p)^{\frac{1}{2}}\boldsymbol{\alpha}$$

- Generalized version of non-linear kinematic hardening rule

- Equation for Backstress falls out naturally from our choice of inelastic stored energy !

- No ad hoc prescription of backstress !

Structure of Rate of Dissipation

$$\zeta_1 = \mathbf{D}_p . \mathbf{K} \mathbf{D}_p ,$$

- Need to prescribe the fourth order tensor **K**
- Dissipation is due to two main reasons:
- Movement of mobile dislocations
  - **K** depends on the density of mobile dislocations
  - According to Gilman (1969)

    Mobile dislocations= $a(s)e^{-\alpha_2 s}$
- Softening due to cavitation in the latter stages of creep.

Rate of Energy Storage

$$\underbrace{\frac{\mathbf{T.L}}{\rho}}_{W_t} = \underbrace{\rho\dot{\psi}}_{W_s} + \underbrace{\zeta_{mech}}_{W_d}$$

$$W_t = W_s + W_d$$

Total Work Done=Work Stored + Work Dissipated

- Each work term arises naturally because of the thermodynamic framework used.
- No ad-hoc coefficients used.
- Instantaneous rate of energy storage, R

$$R = 1 - \frac{W_d}{W_T} = \frac{W_s}{W}$$

Constitutive Model

- Maximization of Rate of Dissipation to determine
  $\mathbf{L}_p = \mathbf{D}_p + \mathbf{W}_p$
- Note: Evolution of natural configuration depends on the driving force

$$\mathbf{A} = p\mathbf{I} + \mathbf{A}^*,$$

$$\mathbf{A}^* = \alpha + \mathbf{K}\mathbf{D}_p + h(s)\frac{\mathbf{D}_p}{(\mathbf{D}_p.\mathbf{D}_p)^{\frac{1}{2}}},$$

$$p = \frac{1}{3}tr(\mathbf{A} - \mathbf{A}^*)$$

$$\mathbf{W}_p = \frac{1}{\eta_2}\boldsymbol{\tau}$$

Results

- The initial results that are presented are obtained using MATLAB.
- Later we will discuss the development of UMAT (User Defined Material Subroutine) and the use of Abaqus to solve boundary value problems for more complex geometries for bodies.

Results

- The problem is solved (for loading along <001>,<111> and <011>) assuming homogeneous deformations with a semi-inverse approach

$$\mathbf{F} = \mathrm{diag}(\phi_1(t), \phi_2(t), \phi_3(t))$$
$$\mathbf{F}_e = \mathrm{diag}(\lambda_1, \lambda_2, \lambda_3)$$
$$\mathbf{G} = \mathrm{diag}(\frac{\phi_1(t)}{\lambda_1}, \frac{\phi_2(t)}{\lambda_2}, \frac{\phi_3(t)}{\lambda_3})$$

- Governing differential equations are obtained using equations for evolution of natural configurations

Material Parameters

ψ_1 : Proportionality constant for inelastic free energy stored in dislocation networks

ψ_2 : Proportionality constant for inelastic free energy due to hardening caused by γ' precipitates

η : Parameter which tells how strongly stored energy depends on deformation history

β_2 : Dislocation multiplication factor

α_1 : Parameter which tell how fast dislocation density saturates

α_2, Ω_2 : Attrition coefficient, related to the fraction of dislocations which are mobile

α_3, Ω_3 : Parameter related to dissipation due to damage accumulation

κ_1, Γ_1 : Parameter which tell how the first mechanism of dissipation depends on driving force

κ_2, Γ_2 : Parameter which tell how the second mechanism of dissipation depends on driving force

β_1, Λ_1 : Proportionality constant for first dissipation mechanism

β_3, Λ_3 : Proportionality constant for second dissipation mechanism

- Model corroborated with <001> & <111> orientations
- 17 Material Parameters (far lesser than crystal plasticity based models)

Anisotropic Creep Results <001>, <011>, <111> directions

- Loading axis can be in an arbitrary direction.
- Requires mapping quantities back and forth between the global and crystal coordinate system.
- Fourth order tensor **K**.

$$\mathbf{K}^{-1} = \begin{bmatrix} i & j & j & 0 & 0 & 0 \\ j & i & j & 0 & 0 & 0 \\ j & j & i & 0 & 0 & 0 \\ 0 & 0 & 0 & k & 0 & 0 \\ 0 & 0 & 0 & 0 & k & 0 \\ 0 & 0 & 0 & 0 & 0 & k \end{bmatrix}$$

Anisotropic Creep, 800^0C, <001>, (CMSX-4)

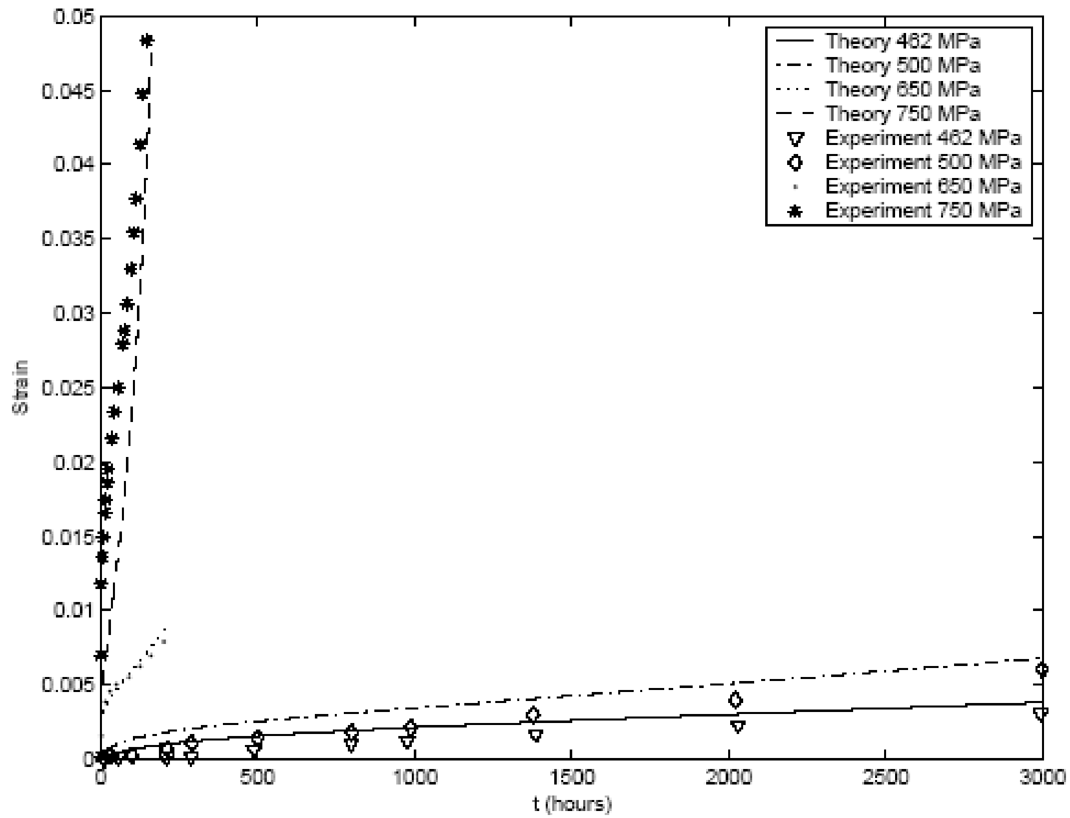

Figure 2: Strain vs. time for CMSX-4 for loading along the <001> orientation, $\theta = 800\ ^oC$: Comparison of the predictions of the model with experimental results of Schubert et al., [24].

Anisotropic Creep, 800^0C, <111>, (CMSX-4)

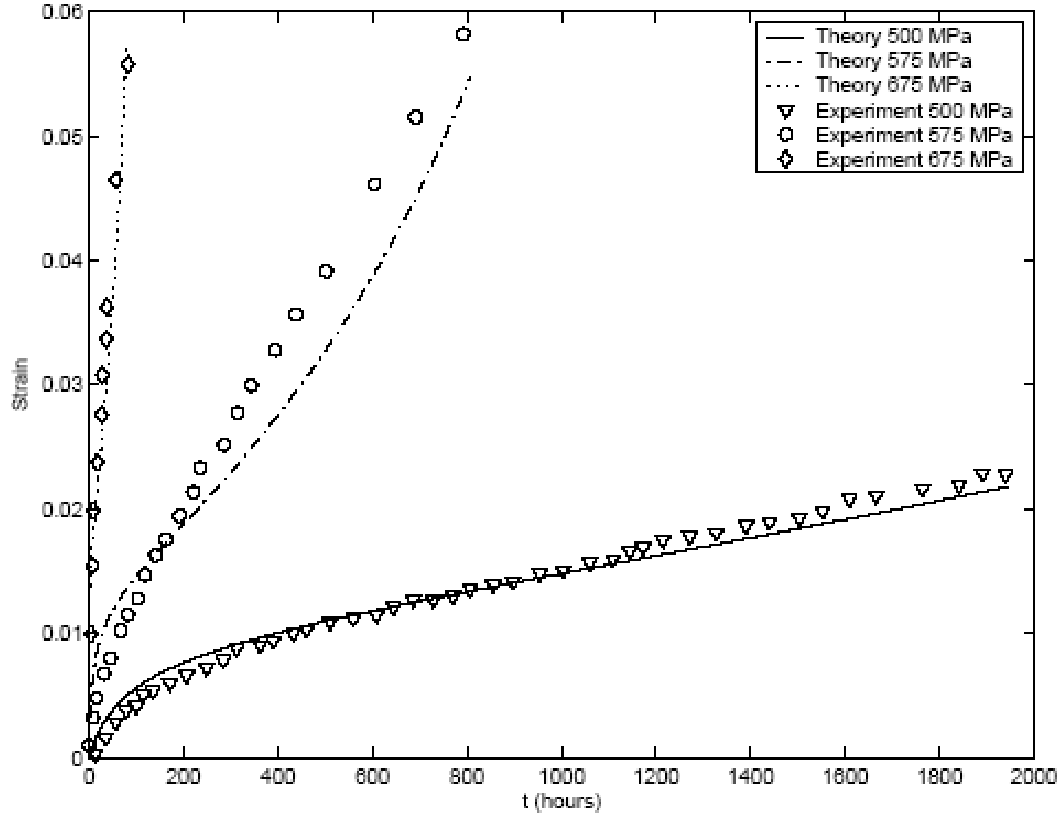

Figure 3: Strain vs. time for CMSX-4 for loading along the <111> orientation, $\theta = 800\ ^o$C: Comparison of the predictions of the model with experimental results of Schubert et al., [24].

Anisotropic Creep, 800^{0}C, <011>, (CMSX-4)

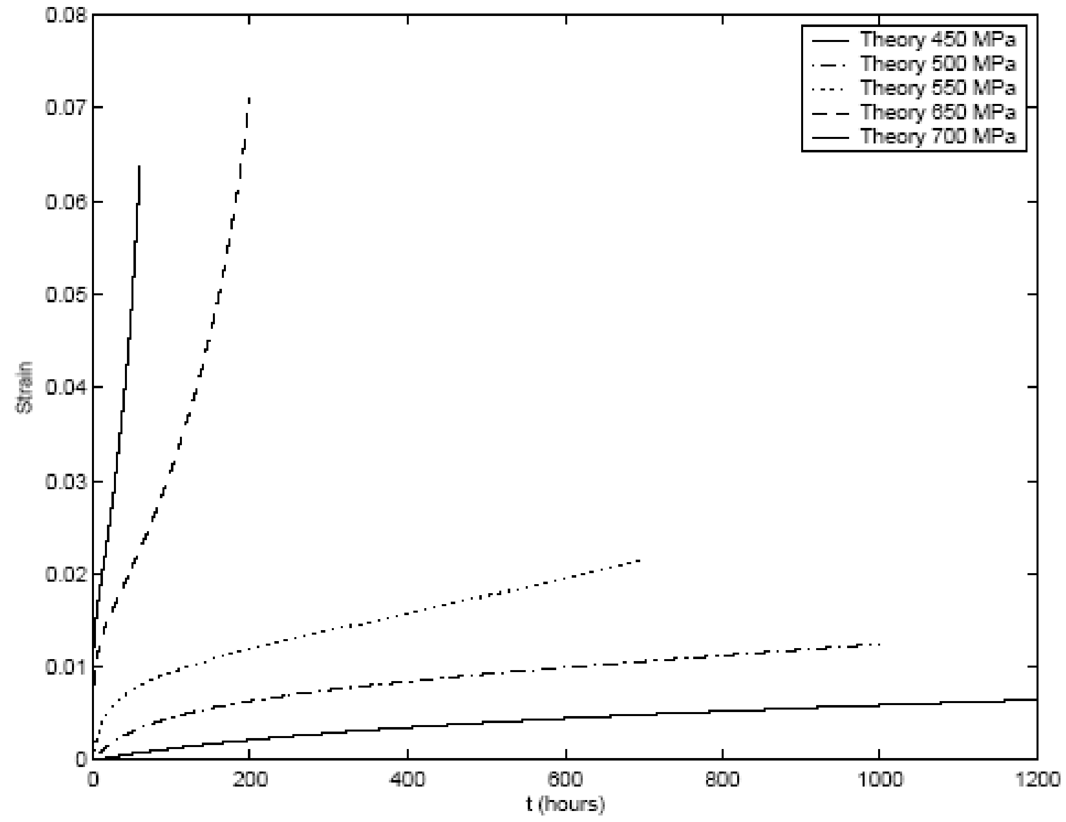

Figure 4: Strain vs. time for CMSX-4 for loading along the <011> orientation, $\theta = 800\ ^oC$.

Predictions of the model !!

Anisotropic Creep, 950^{0}C, <001>, (CMSX-4)

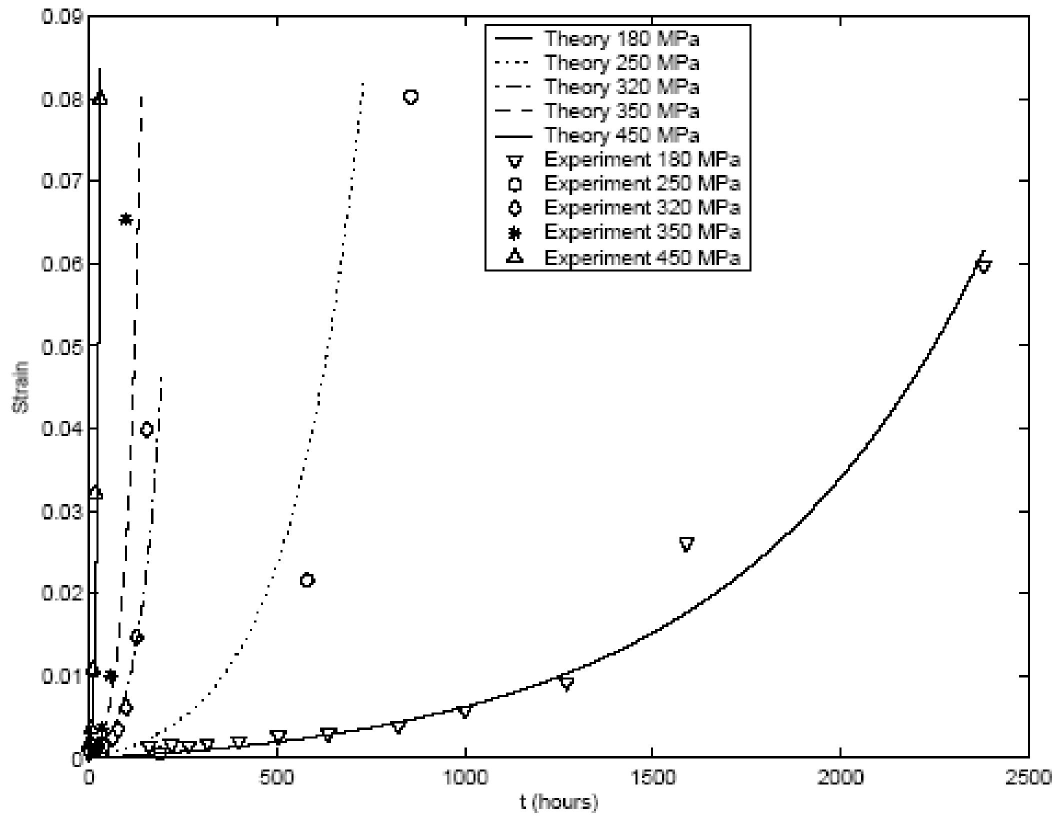

Figure 5: Strain vs. time for CMSX-4 for loading along the <001> orientation, $\theta = 950\ ^oC$: Comparison of the predictions of the model with experimental results of MacLachlan et al., [25].

Anisotropic Creep, 950^0C, <111>, (CMSX-4)

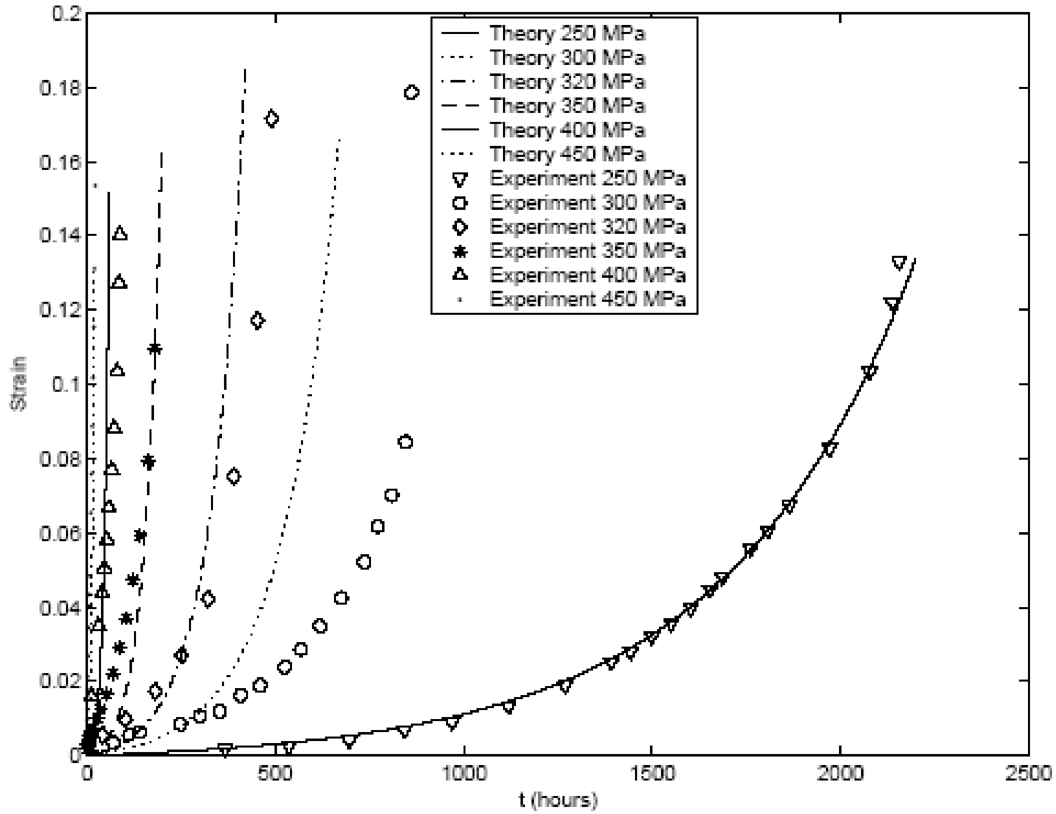

Figure 6: Strain vs. time for CMSX-4 for loading along the <111> orientation, $\theta = 950\ ^oC$: Comparison of the predictions of the model with experimental results of MacLachlan et al., [25].

Anisotropic Creep, 950^{0}C, <011>, (CMSX-4)

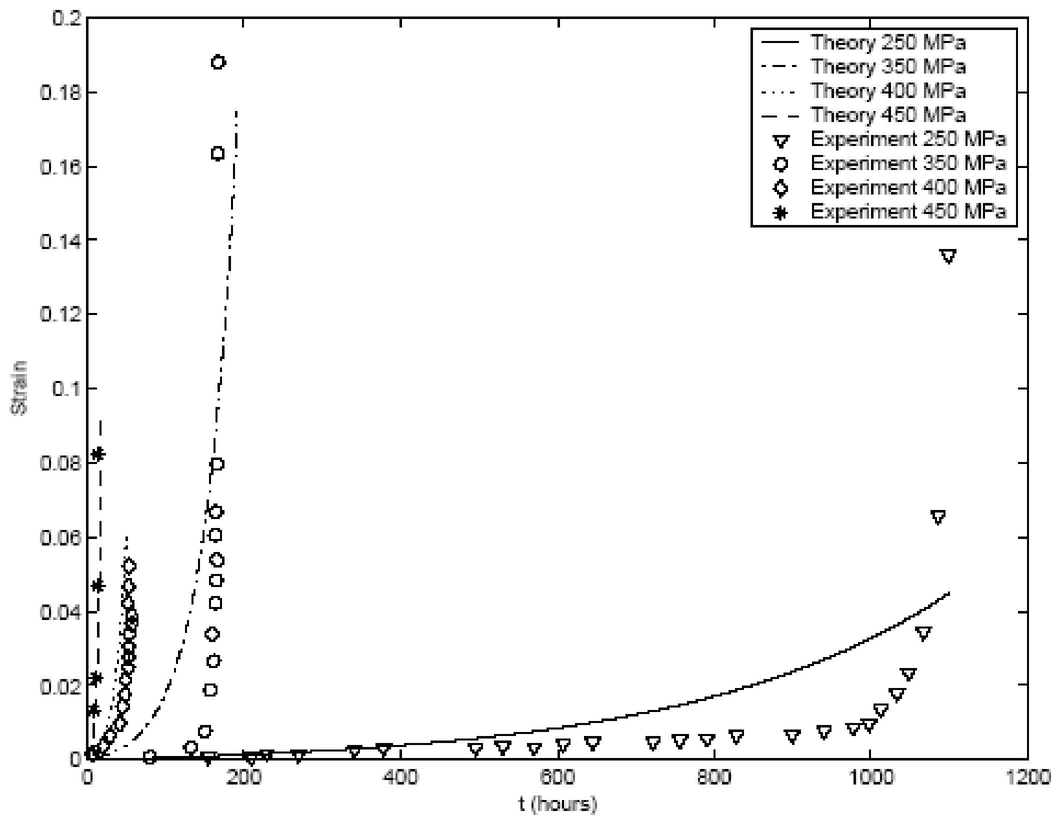

Figure 7: Strain vs. time for CMSX-4 for loading along the <011> orientation, θ = 950 °C: Comparison of the predictions of the model with experimental results of MacLachlan et al., [25].

Model corroborated with <001> & <111> predicts <011> well !!

Finite Element Implementation

- Large deformation
- Coupled Non-linear Partial Differential Equations
- Newton's Method to solve the non-linear problem at each iteration.
- Implicit Scheme to enable large time steps
- Need to Specify the tangent stiffness matrix
  - To ensure quadratic rate of convergence.
  - Satisfy incremental objectivity (numerical solution will be frame invariant).
- Implemented using ABAQUS through the development of a user defined subroutine UMAT.

Computational Subroutines in Abaqus

- The constitutive model has been implemented in Abaqus/Standard through UMAT

ABAQUS

•Solves the equilibrium equation at every time step (quasi-static problem)

• Large deformation analysis is carried out

$$\mathbf{F}(t), \mathbf{F}(t+\Delta t)$$

$$\mathbf{F}_e(t), \mathbf{T}(t), s(t), \mathbf{G}(t)$$

UMAT

•Evaluates various quantities at time t+dt using their values at time t.

•Uses an implicit scheme based on backward difference (backward Euler Method).

•Solves the resulting non-linear equation using Newton-Raphson method

$$\mathbf{F}_e(t+\Delta t), \mathbf{T}(t+\Delta t)$$

$$s(t+\Delta t), \mathbf{G}(t+\Delta t)$$

Numerical Scheme in UMAT

- Numerical scheme based on first order backward difference (implicit scheme, unconditionally stable)

First Order Backward Difference

$$f_1 := {}^{t+\Delta t}s - {}^{t}s - \Delta t\sqrt{\left({}^{t+\Delta t}\mathbf{D}_p \,.\, {}^{t+\Delta t}\mathbf{D}_p\right)} = 0$$

$$\boldsymbol{f}_2 := {}^{t+\Delta t}\mathbf{D}_p - \left({}^{t+\Delta t}\bar{\mathbf{K}}\right)^{-1}\left({}^{t+\Delta t}\mathbf{A} - \frac{1}{3}tr({}^{t+\Delta t}\mathbf{A})\mathbf{1} - {}^{t+\Delta t}\boldsymbol{\alpha}\right) = \mathbf{0}$$

$$\boldsymbol{f}_3 := {}^{t+\Delta t}\boldsymbol{\alpha} - {}^{t}\boldsymbol{\alpha} - \rho\psi_2\Delta t\, {}^{t+\Delta t}\mathbf{D}_p + \eta\, {}^{t+\Delta t}\boldsymbol{\alpha}\left({}^{t+\Delta t}s - {}^{t}s\right) = \mathbf{0}$$

$$f_4 := {}^{t+\Delta t}\tilde{\psi} - {}^{t}\tilde{\psi} - \frac{h(s)}{\rho}\left({}^{t+\Delta t}s - {}^{t}s\right) - \Delta t\, {}^{t+\Delta t}\boldsymbol{\alpha} \,.\, {}^{t+\Delta t}\mathbf{D}_p = 0$$

Numerical Scheme in UMAT

Need to find solution to $\boldsymbol{F}(\boldsymbol{X}) = \{\mathbf{0}\}$

$$\boldsymbol{F} = \begin{Bmatrix} f_1 \\ \boldsymbol{f}_2 \\ \boldsymbol{f}_3 \\ f_4 \end{Bmatrix} \quad \boldsymbol{X} = \begin{Bmatrix} {}^{t+\Delta t}s \\ {}^{t+\Delta t}\mathbf{D}_p \\ {}^{t+\Delta t}\boldsymbol{\alpha} \\ {}^{t+\Delta t}\tilde{\psi} \end{Bmatrix} \quad [J] = \frac{\partial \boldsymbol{F}}{\partial \boldsymbol{X}}$$

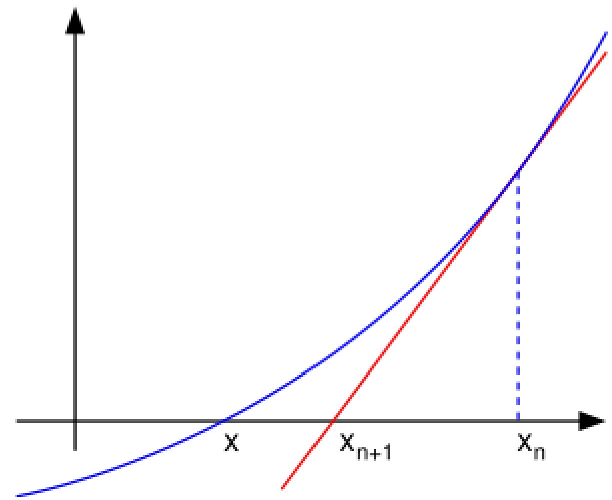

Use Newton Raphson Scheme

$$\boldsymbol{X}^{k+1} = \boldsymbol{X}^{k} - [J]^{-1}\boldsymbol{F}(\boldsymbol{X}^{k}) \,, \quad k - \text{iteration number}$$

Update of $\mathbf{G}$ (Eterovic and Bathe (1990))

$${}^{t+\Delta t}\mathbf{G} = \exp(\Delta t\, {}^{t+\Delta t}\mathbf{L}_p)\, {}^{t}\mathbf{G}$$

Update on $\mathbf{F}_e$

$${}^{t+\Delta t}\mathbf{F}_e = {}^{t+\Delta t}\mathbf{F}\left({}^{t+\Delta t}\mathbf{G}\right)^{-1}$$

Computational Subroutines in Abaqus

- Inelastic strain pathlength s , and tensor $\mathbf{G}$ are stored as solution dependent variables (SDV)
- Initial conditions on solution dependent variables (SDV) are imposed through User Routine SDVINI in Abaqus/Standard
- Orientation of crystal lattice is imposed through User Routine ORIENT in Abaqus/Standard

Validation of Abaqus UMAT

- The UMAT for our constitutive model has been validated by comparing results for cases with available experimental results

- Elaborate testing of the UMAT is done for a variety of cases to validate its efficacy

Comparision of Results, Strain (CMSX-4 , 750 ºC, <001>, Svoboda & Lucas (1998))

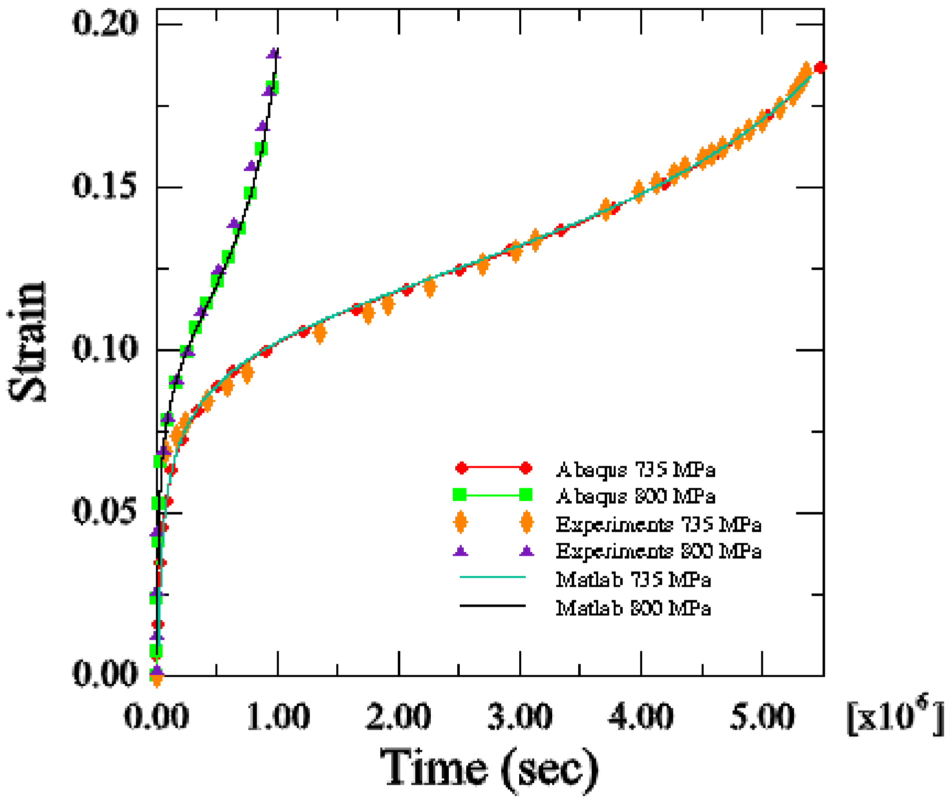

Comparision of Results, Strain (CMSX-4, 982 ^oC, <001> Henderson & Lindblom (1997),)

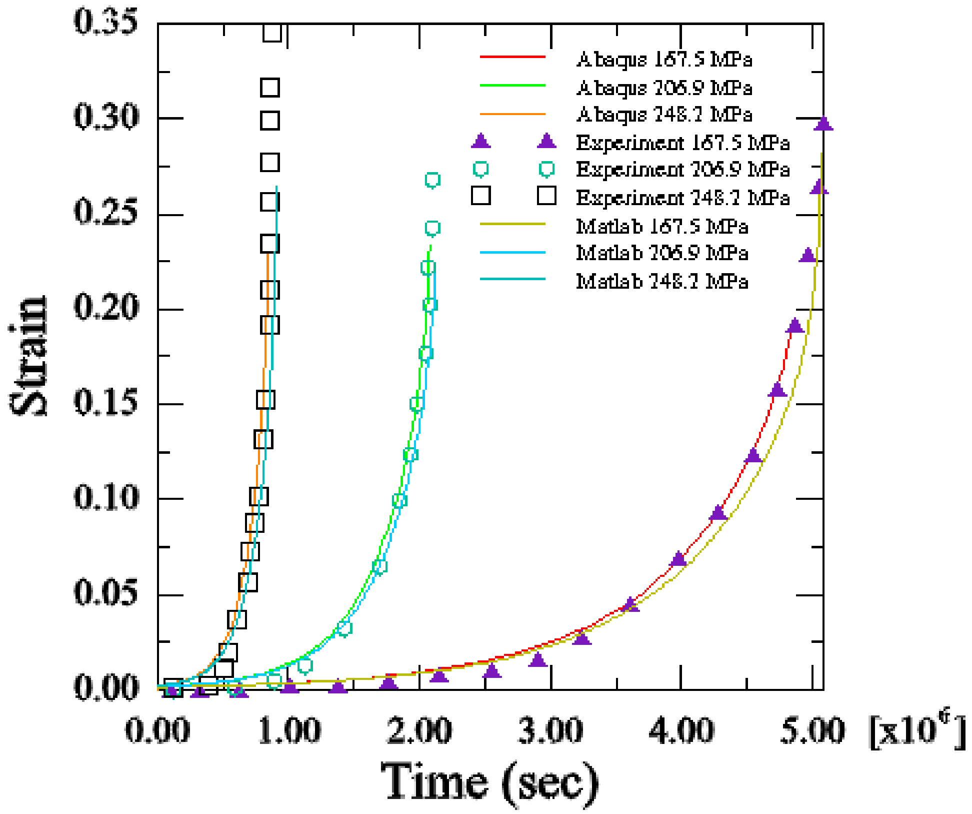

Comparision of Results (CMSX-4, <001>, 1000 ºC, Svoboda & Lucas (1998),)

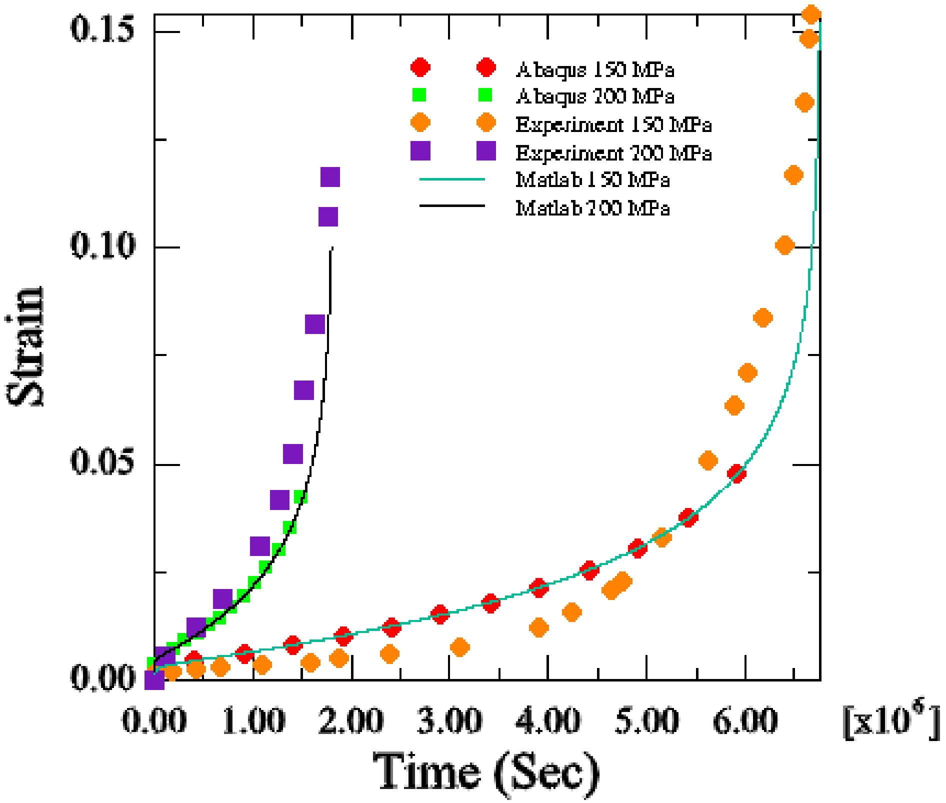

Comparision of Results, Inelastic Stored Energy (CMSX-4, <001>, 750 ^{o}C)

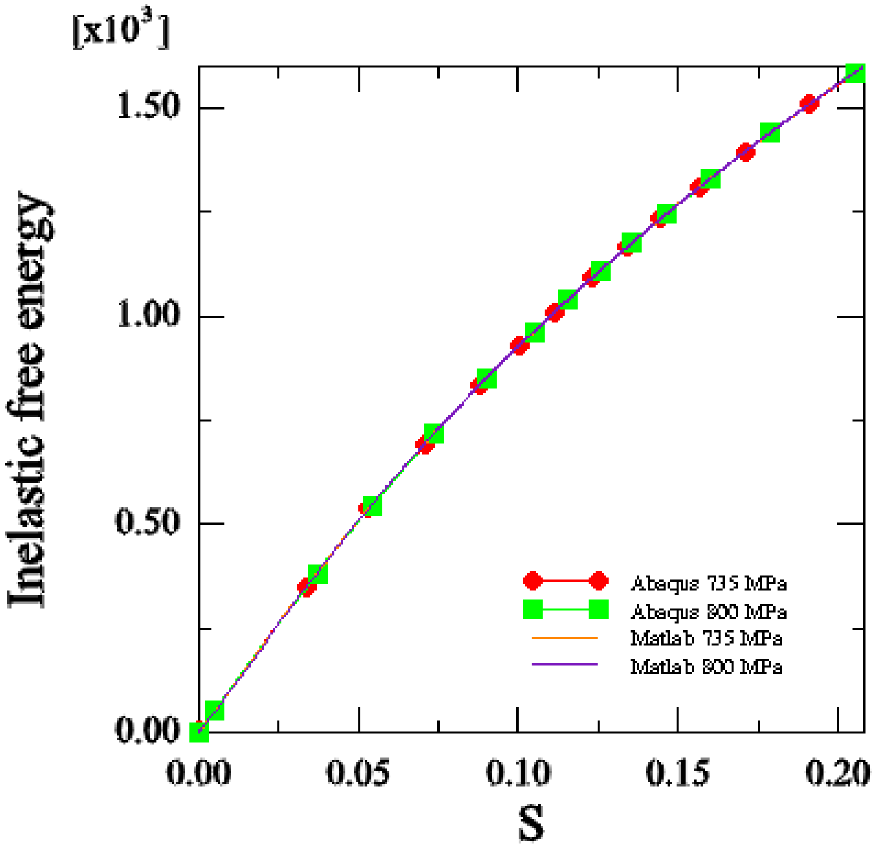

Comparision of Results, Ws/Wp (CMSX-4, <001>, 750 ºC,)

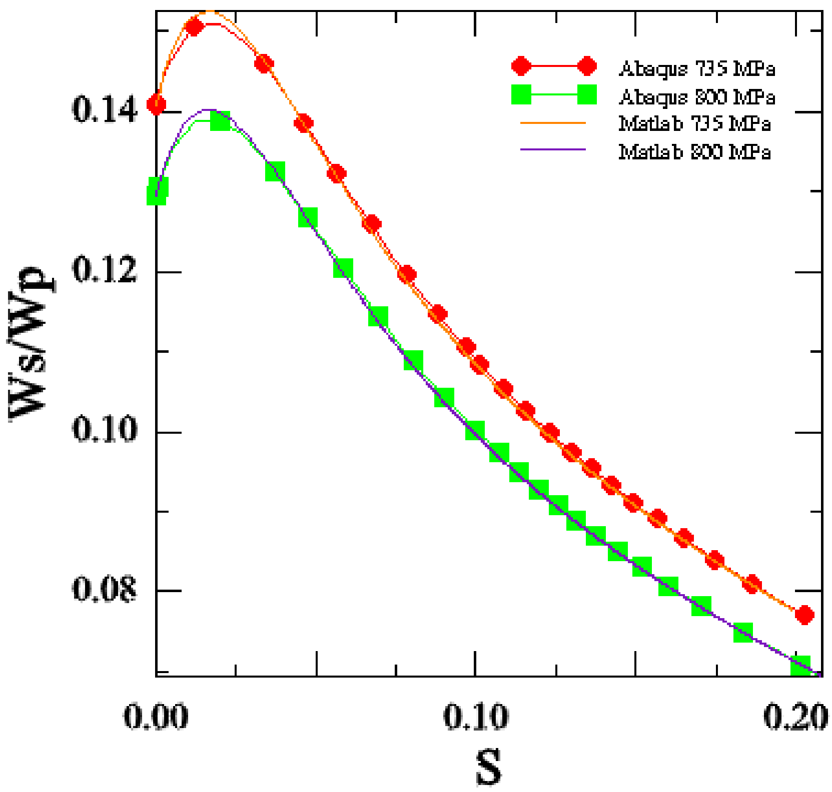

Comparison of Results

- The model has been implemented in ABAQUS/STANDARD through User Defined Routines (UMAT, SDVINI, ORIENT)

- Experimental results, results obtained in MATLAB and results obtained in ABAQUS agree well

- First order implicit backward difference method implemented in UMAT is stable although time steps need to be controlled to achieve accurate results

Inhomogeneous Deformation of a <001> Oriented Creep Specimen

- UMAT is used to study inhomogeneous deformation of a creep specimen
- 800 ^{o}C, <001> Oriented
- Boundary Conditions: Uniform tensile loading (200 MPa) along the top surface

  Bottom Plane is fixed in space

Typical Finite Element Mesh

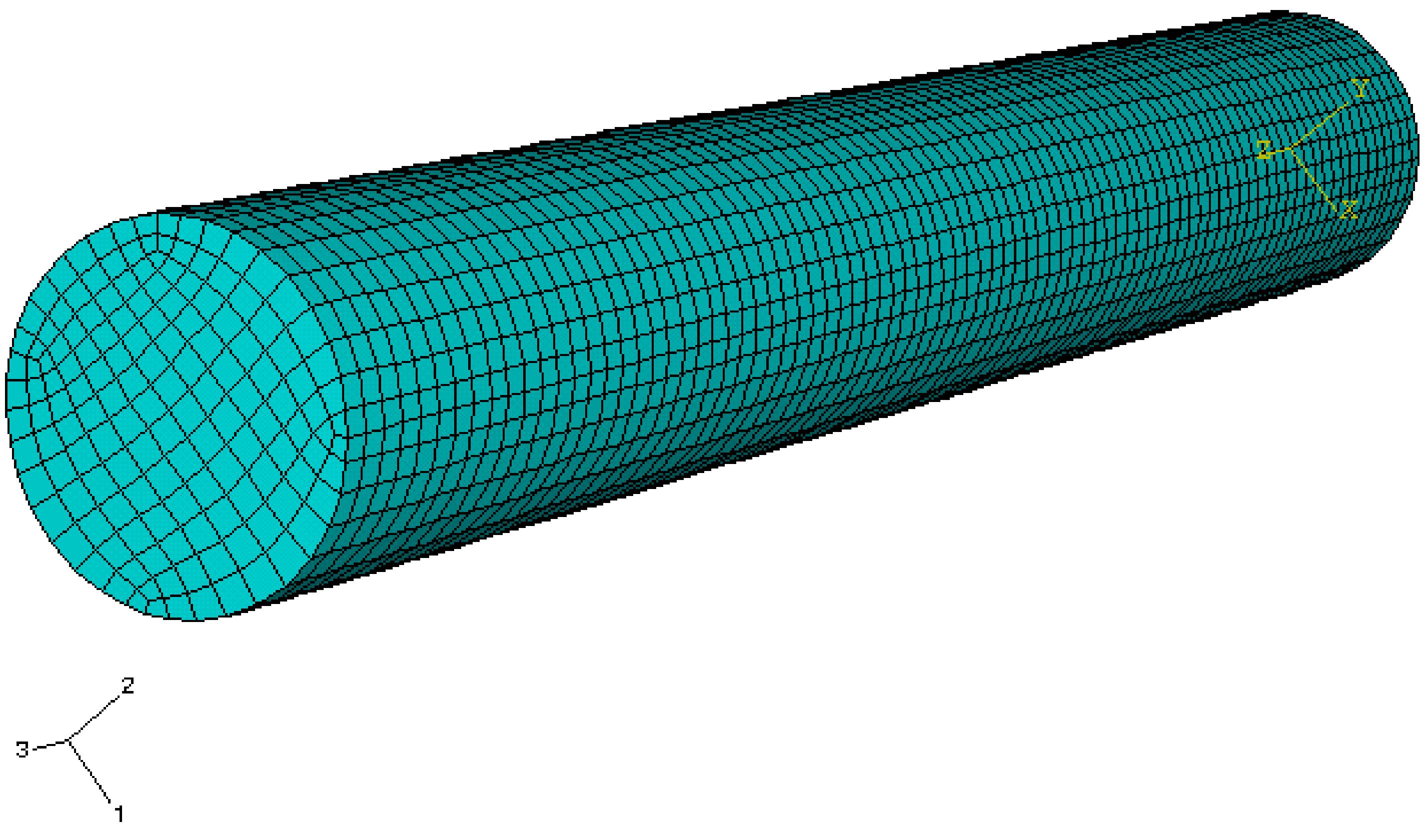

Inhomogeneous Deformation of a <001> Oriented Creep Specimen

- Stresses after 1) initial elastic step

  2) after creep for 4.6E6 Secs (~1280 hours)

1)

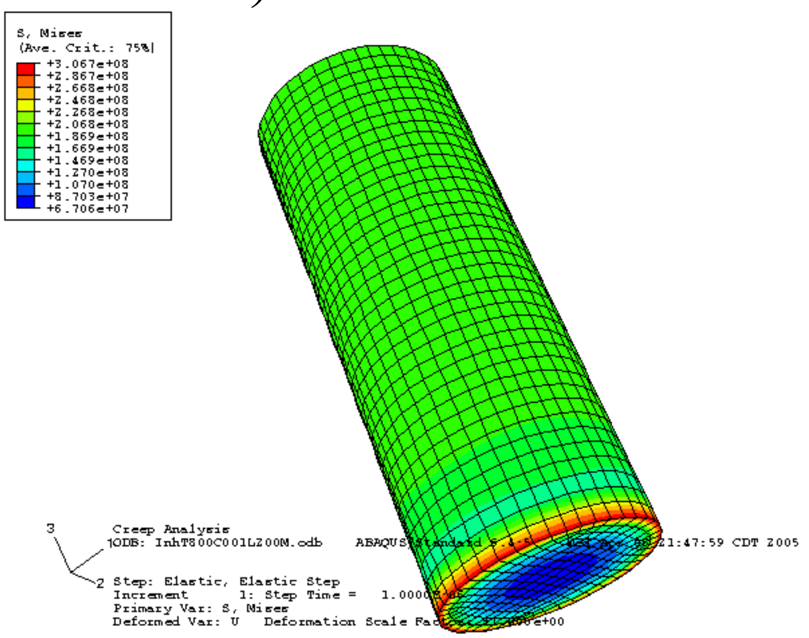

(2)

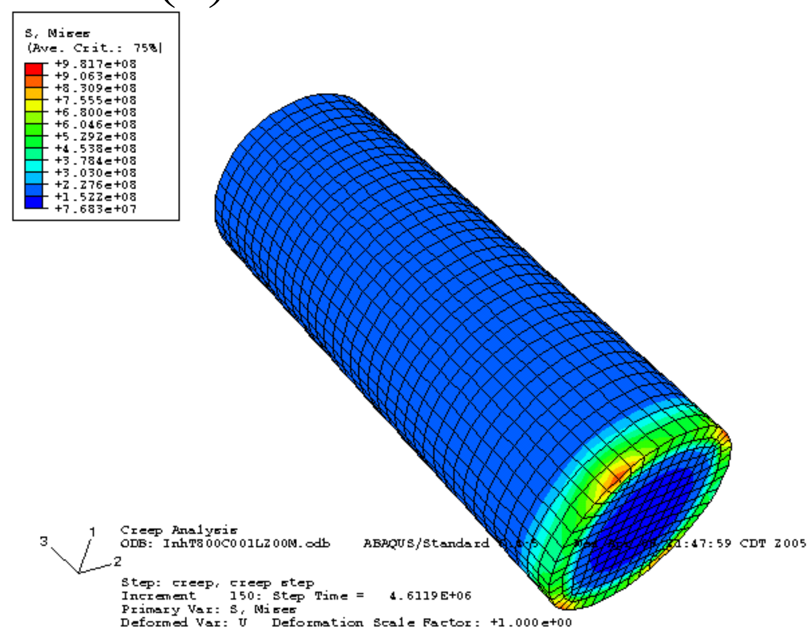

Inhomogeneous Deformation of a <001> Oriented Creep Specimen

- Strain in various regions of stresses due to creep

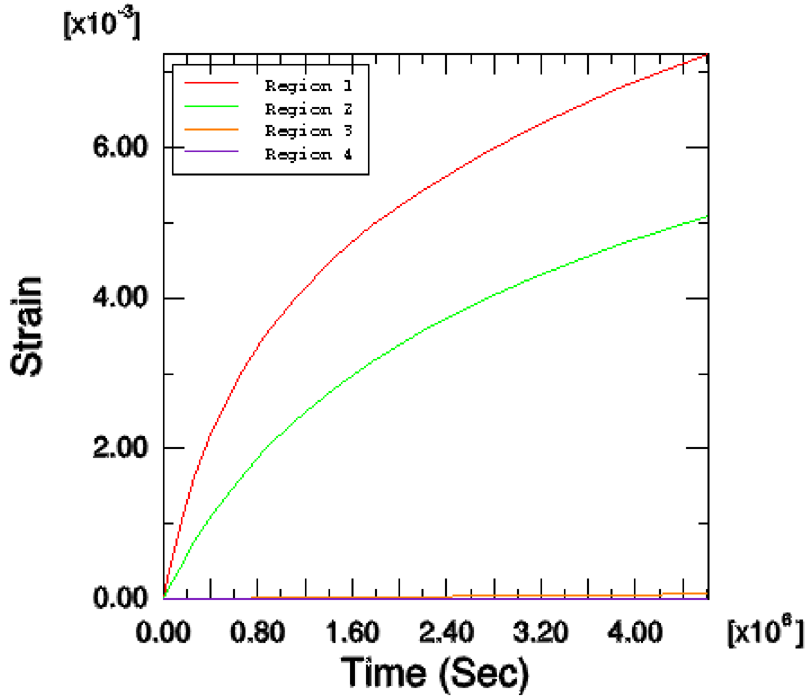

Homogeneous Deformation of Turbine blade

- UMAT has been tested for Homogeneous deformation of a turbine blade at 800 ^{o}C, <001> Oriented

- Boundary conditions: Uniform loading (800 MPa) on top surface,

  Bottom plane remain fixed in z direction (the direction of blade axis),

  One point on the bottom plane near the leading edge is fixed in space

Homogeneous Deformation of Turbine blade

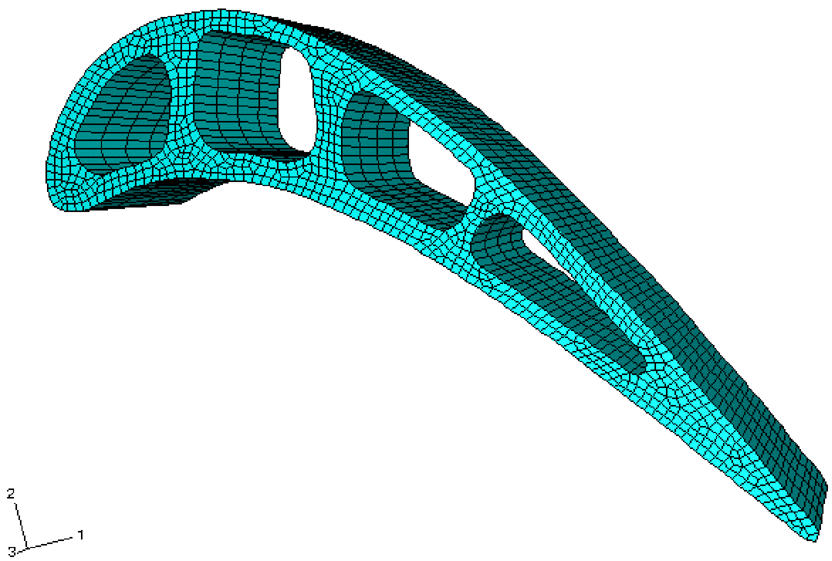

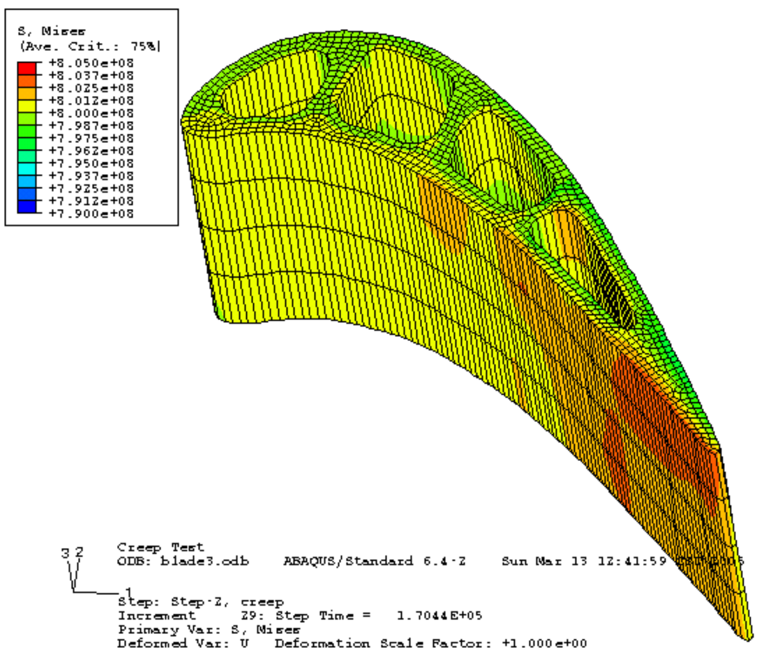

Homogeneous Deformation of Turbine blade

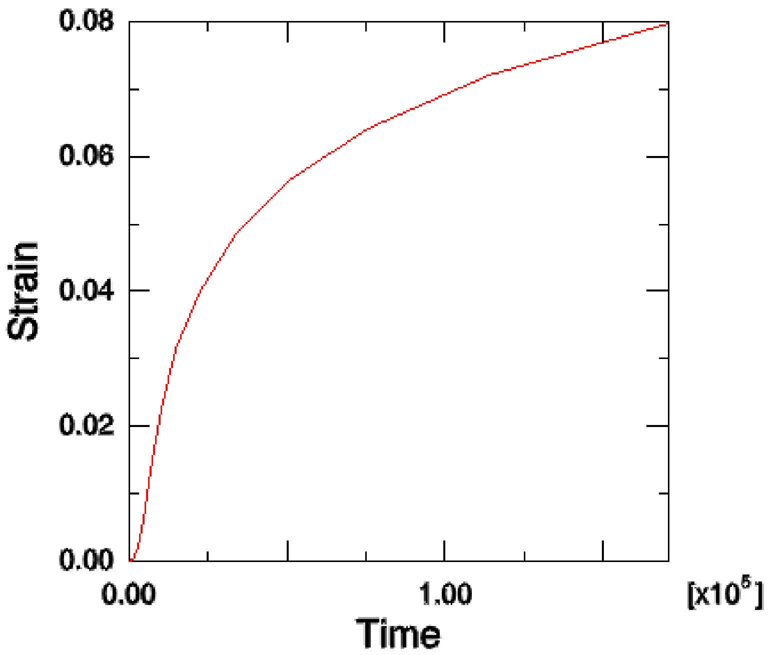

Conclusion

- Development of constitutive model for creep has been successfully completed
- The model is successful in predicting creep behavior for
  - a range of temperatures pertinent to gas turbine blade applications (750 ^{o}C - 1000 ^{o}C)
  - a range of loads
  - loading in different orientations (<001>, <111> and <011>)

Conclusion

- The constitutive model has been implemented in Abaqus/Standard through UMAT
- The UMAT has been validated with experimental results and results for the case of a homogeneous deformation
- The UMAT is able to solve for complex deformations

Future Work

- Pick desired properties
- Use computational results from Abaqus to vary choice of material functions.
- Optimize choice of stored energy, rate of entropy production to engineer specific properties

Thank You

Comparision of Results, Backstress (CMSX-4, <001>, 750 ºC,)

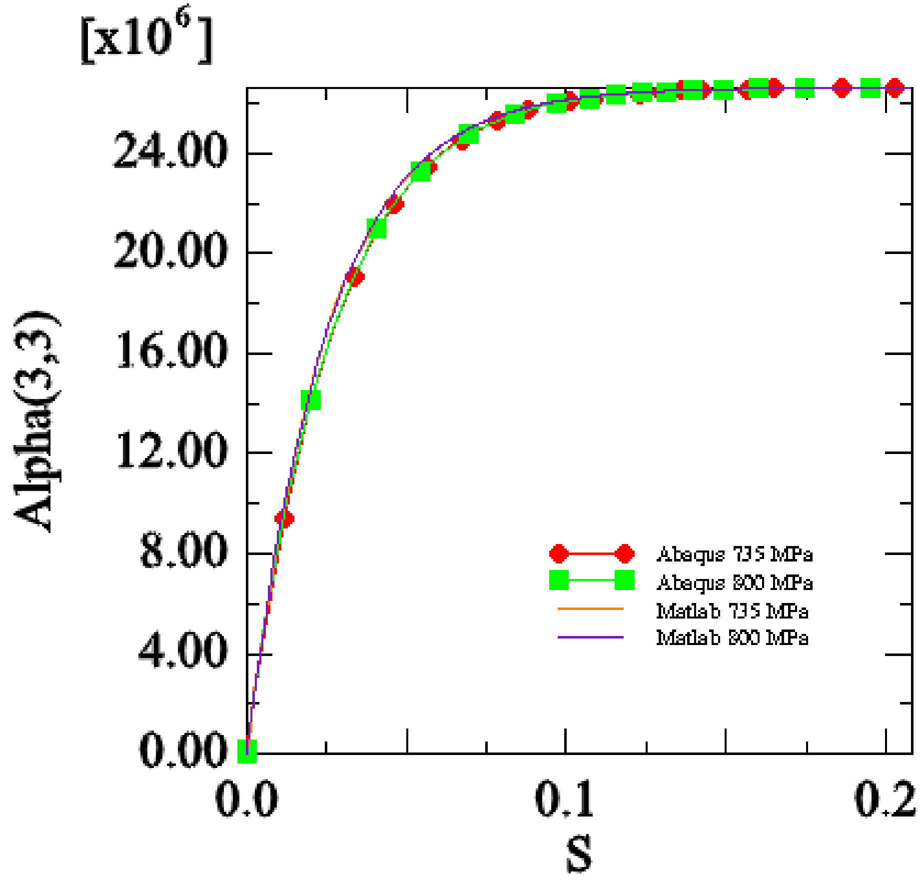

Comparision of Results, Backstress (CMSX-4, <001>, 982 ºC,)

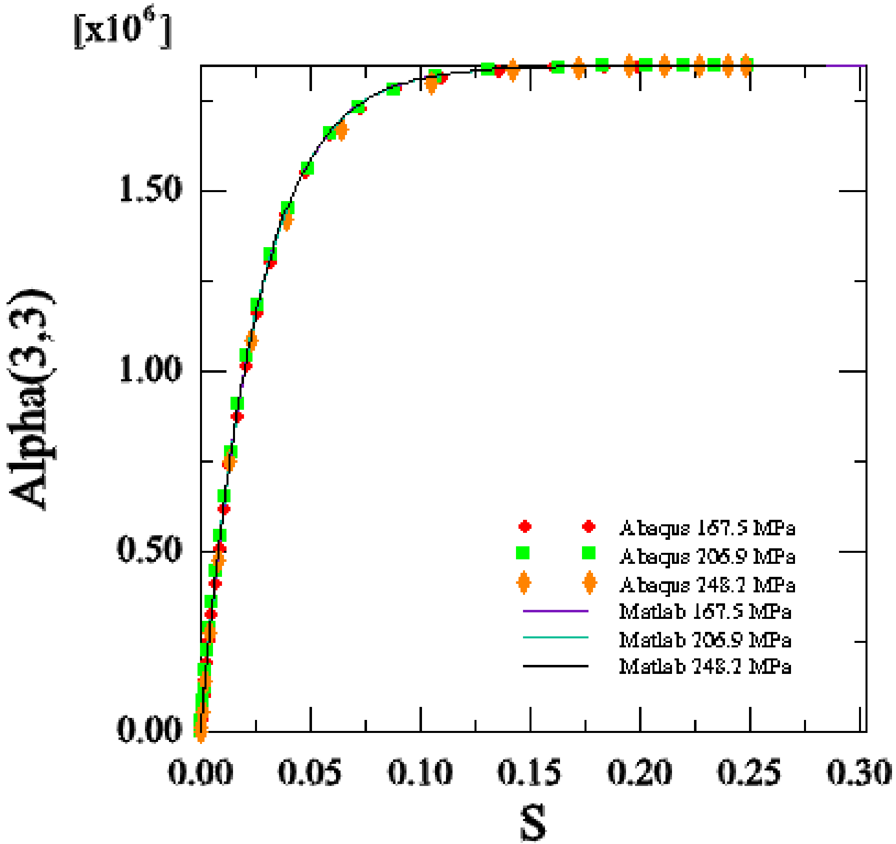

Comparision of Results, Inelastic Stored Energy (CMSX-4, <001>, 982 ^{o}C)

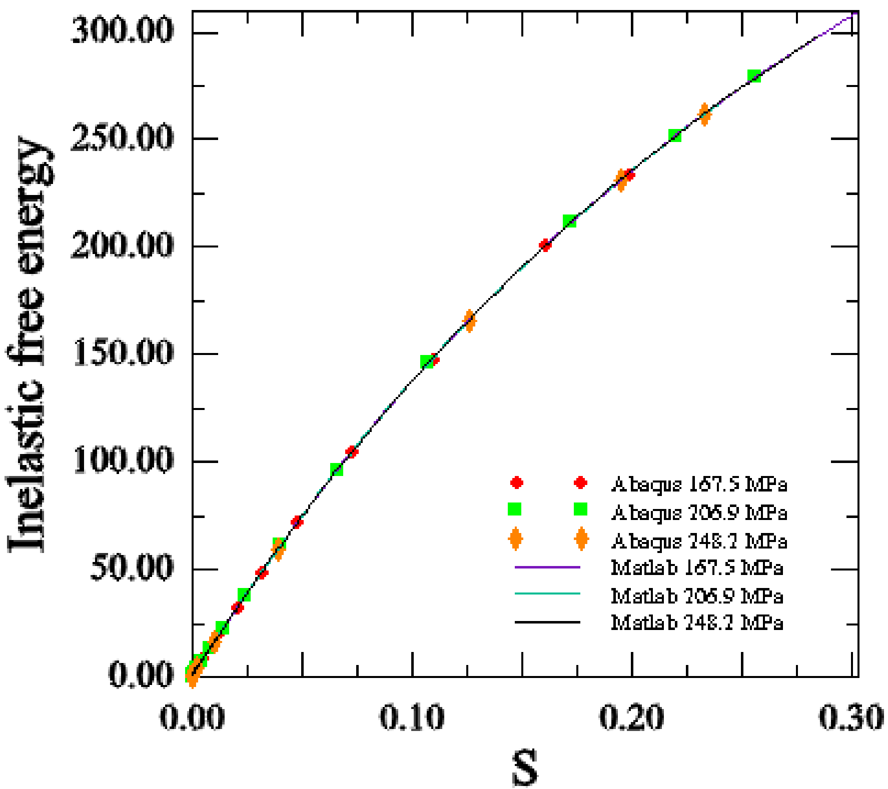

Comparision of Results, Ws/Wp (CMSX-4, <001>, 982 ºC)

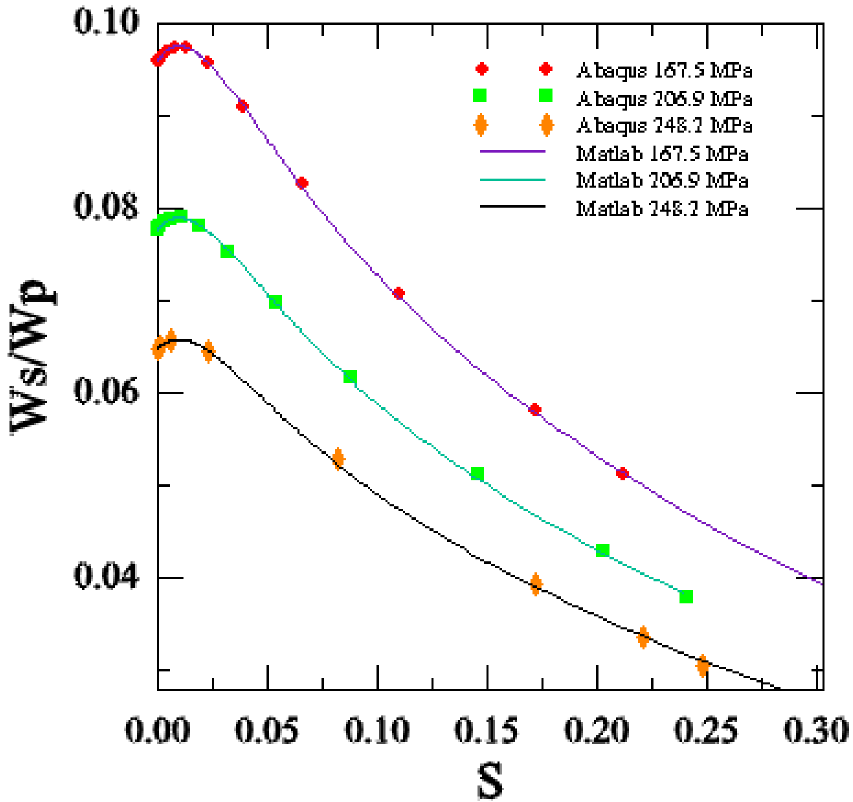

Comparision of Results, Backstress (CMSX-4, <001>, 1000 ^oC,)

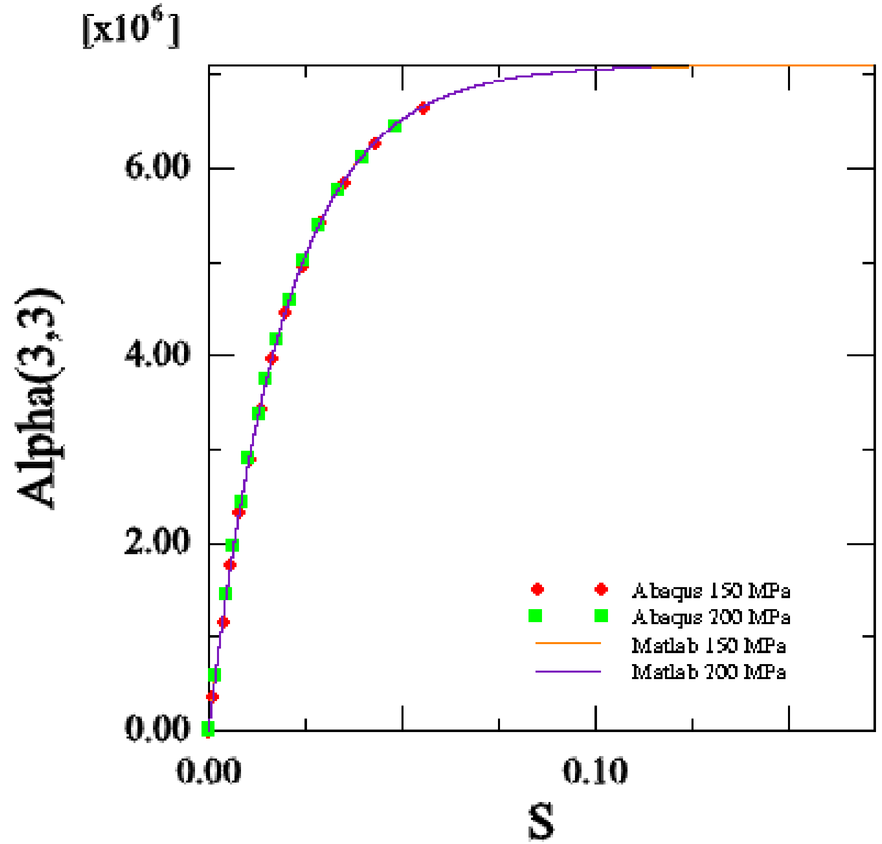

Comparision of Results, Inelastic Stored Energy (CMSX-4, <001>, 1000 ^oC)

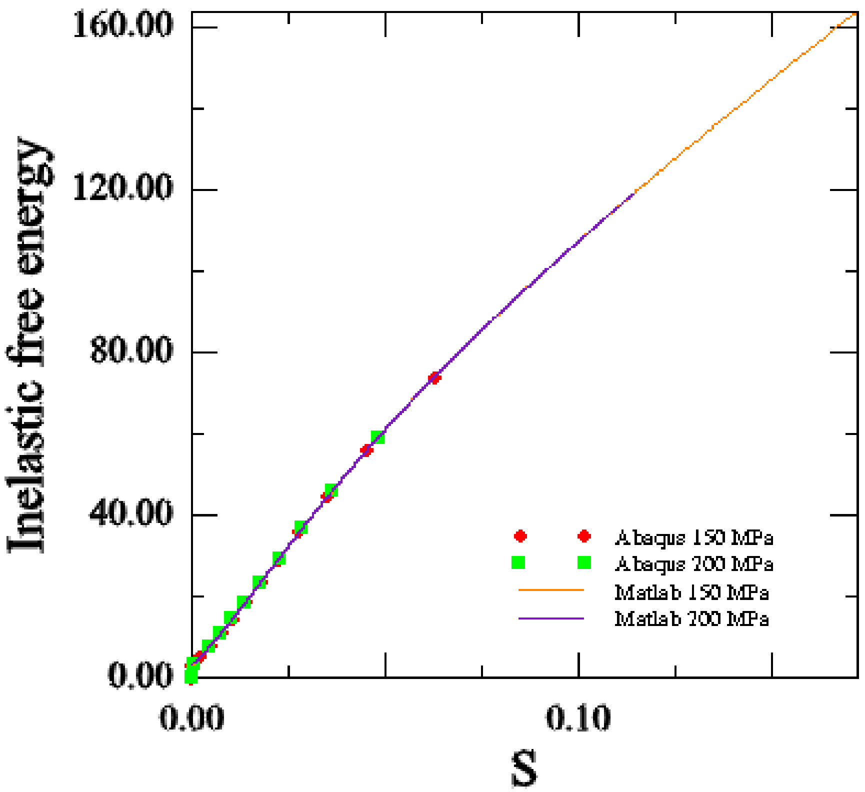

Comparision of Results, Ws/Wp (CMSX-4, <001>, 1000 ^oC,)

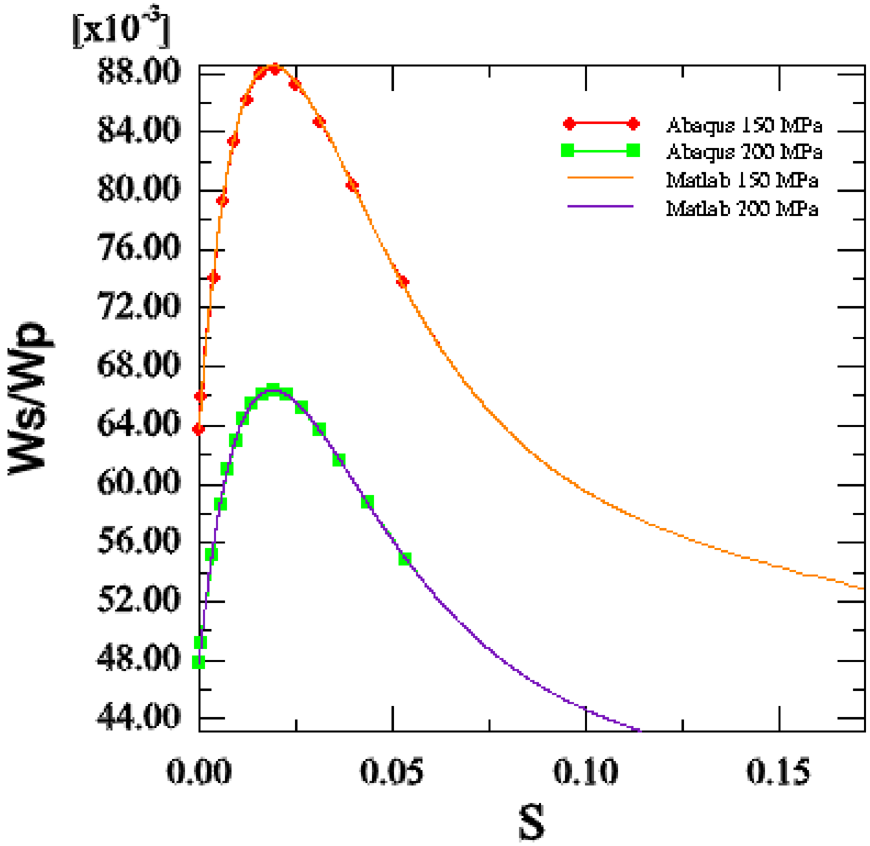

Comparision of Results, Backstress (CMSX-4, <001>, 1000 ºC,)

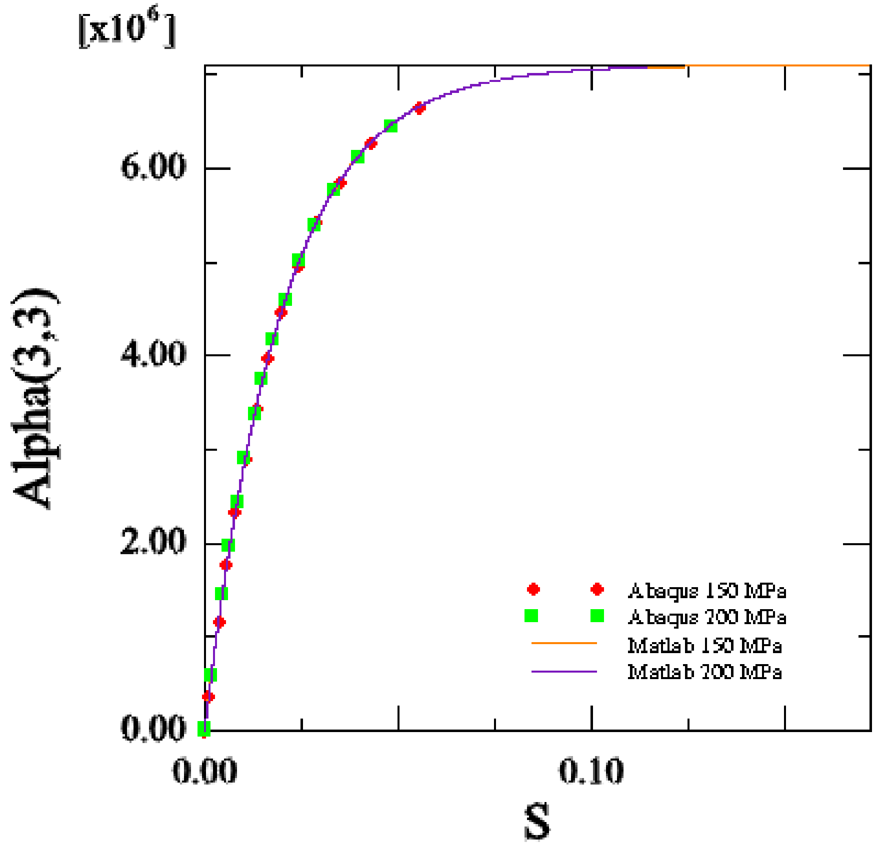

Comparision of Results, Inelastic Stored Energy (CMSX-4, <001>, 1000 ^oC)

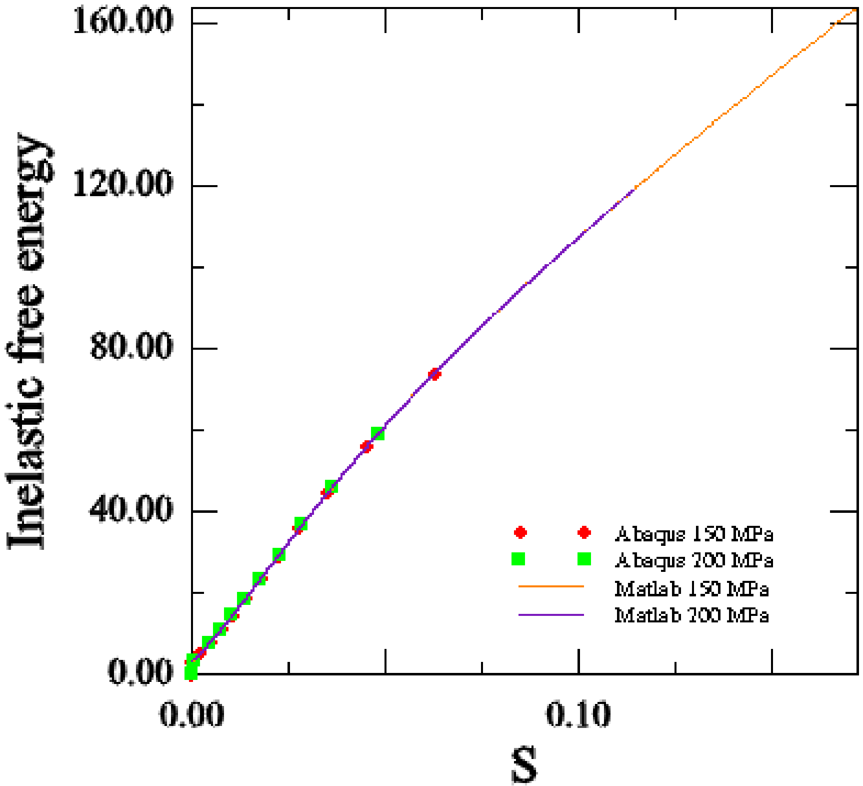

Comparision of Results, Ws/Wp (CMSX-4, <001>, 1000 ^oC,)

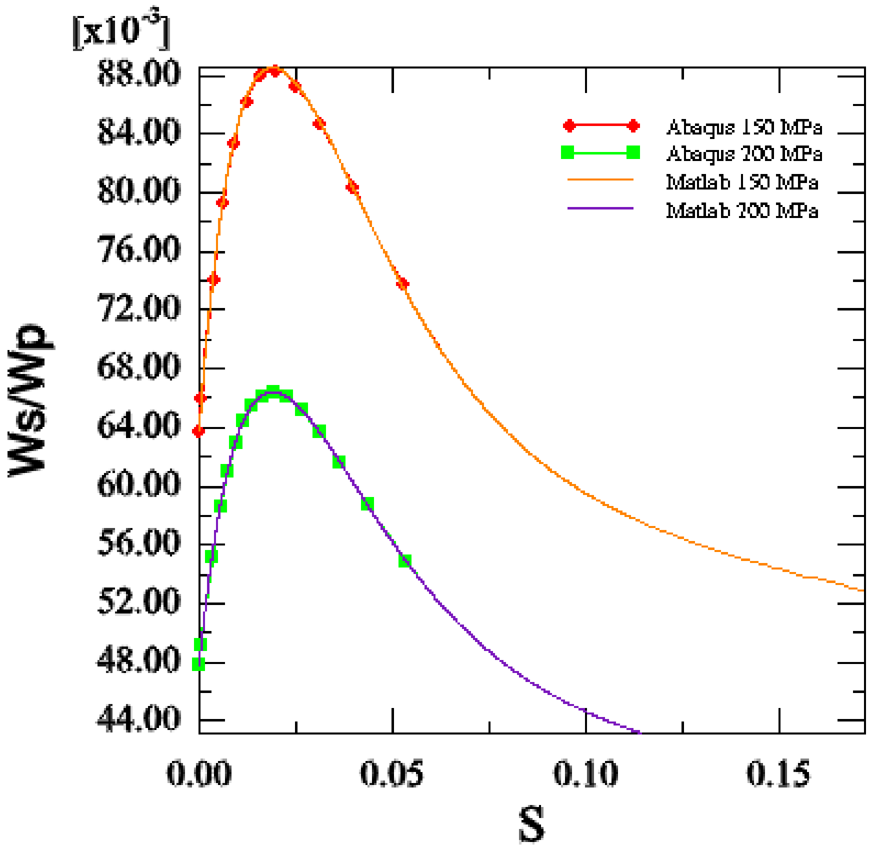

Conclusion

- The model is within a thermodynamic setting and takes into account the anisotropy associated with single crystal and its evolution with inelastic strain

- The model takes into account the microstructure of single crystal superalloys, motion of dislocations and their interaction with secondary precipitates

Homogeneous Deformation of Turbine blade

- UMAT has been tested for Homogeneous deformation of a turbine blade at 800 ^{o}C, <001> Oriented

- Boundary conditions: Uniform loading (800 MPa) on top surface,

  Bottom plane remain fixed in z direction (the direction of blade axis),

  One point on the bottom plane near the leading edge is fixed in space

Typical Composition of Nickel Based Single Crystal Superalloys

	Ni	Cr	Co	Mo	W	Al	Ti	Ta	Re	Nb	V	Hf
First Generation												
Rene N4	62.6	9	8	2	6	3.7	4.2	4		0.5		
CMSX-2	66.6	8	4.6	0.6	7.9	5.6	0.9	5.8				
Second Generation												
Rene N5	61.8	7	8	2	5	6.2		7	3			0.2
CMSX-4	61.8	6.5	9	0.6	6	5.6	1	6.5	3			0.1
Third Generation												
Rene N6	57.4	4.2	12.5	1.4	6	5.75	0	7.2	5.4	0	0	0.15
CMSX-10	69.6	2	3	0.4	5	5.7	0.2	8	6	0.1		0.03

Homogeneous Deformation of Turbine blade